

APPENDIX 2G

GEOTECHNICAL STABILITY ANALYSES

For inspection purposes only.
Consent of copyright owner required for any other use.

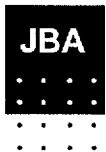
ROADSTONE DUBLIN LIMITED

**REMEDICATION OF UNAUTHORISED LANDFILL SITES
AND DEVELOPMENT OF ENGINEERED LANDFILL,
BLESSINGTON, CO. WICKLOW**

SLOPE STABILITY ASSESSMENT

December 2004

*For inspection purposes only.
Consent of copyright owner required for any other use.*



Prepared by :
John Barnett and Associates /
SLR Consulting
7 Dundrum Business Park
Windy Arbour
Dublin 14



Prepared for :
Roadstone Dublin Ltd.
Fortunestown
Tallaght
Dublin 24

SLOPE STABILITY ASSESSMENT

1.0 Introduction

The following report details the investigation of the stability of the lining system for the proposed engineered landfill at Blessington, Co. Wicklow. The design incorporates the lining of the 1v:3h perimeter slope of the landfill, using geosynthetic materials.

2.0 Brief Background to Stability Issues

The engineered landfill is located within an active sand and gravel quarry and is intended to be used to contain waste that has been illegally disposed of at the site. The existing quarried faces at the site currently stand at angles in excess of 45° and show no signs of mass instability. Given the stability of the current slopes on site and the nature of the geology, the global stability of the perimeter slopes of the engineered landfill (1v:3h) is not considered in this report. The focus of this report therefore centres on the stability at the interfaces of the geosynthetic elements of the lining system to be installed in their unconfined condition, i.e. prior to waste placement.

The proposed lining system to the side slopes at Blessington comprises the following elements, from the top down:

- 500mm thick Leachate Drainage Blanket
- Geotextile Protector
- 2mm Thick Textured Geomembrane
- Geosynthetic Clay Liner (GCL)
- 1m Thick Clay Liner

3.0 Method of Analysis and Approach

The stability of geosynthetic lining systems is controlled by the shear resistance available at the various interfaces, i.e. geomembrane / geotextile, within the lining system. In the hypothetical scenario of an infinitely long slope and purely frictional materials, i.e. no cohesion, the factor of safety is calculated simply by dividing the tangent of the angle of shear resistance by the tangent of the angle of the slope.

However, in the reality the calculation of the factor of safety is dependant upon other factors, including:

- The cohesive element of the interface shear strength;
- The degree of saturation of overlying soils;
- The length over which the soils are placed;
- The passive resistance provided by the soils at the toe of the slope.

The method of analysis used in the investigation of interface stability was proposed by Jones and Dixon (Reference 1). This method incorporates all of the above factors when considering the stability of the lining system. The method of analysis calculates the factor of safety against failure of the overlying soils and each interface in the system, and allows the calculation of tension within each geosynthetic element of the lining system. Relevant sections of the Jones and Dixon paper detailing the equations used to calculate the factor of safety and the tension within the system are attached in Appendix I.

In order to model the performance of the lining system under loading, a Mohr-Coulomb failure criterion is adopted to define the angle of shearing resistance and the cohesion intercept for each interface. In the absence of actual data for the materials to be used, values have been adopted in the analysis from published data. These values are considered to be conservative and are detailed in Table 1 below.

The cohesion intercept of the mineral liner geotextile intercept has been reduced (compared to the published data) in order to model the softening of the soil immediately adjacent to the permeable boundary formed by the geotextile.

Element of Lining System	Angle of Shearing Resistance degrees (°)	Cohesive Intercept (kPa)
Leachate drainage blanket	35	0
Drainage Blanket / Geotextile Protector Interface	30	0
Geotextile / Textured Geomembrane Interface	26	7
Textured Geomembrane / GCL	25	2
GCL / Mineral Liner Subgrade Interface	23	2

Table 1 : Summary of Shear Strength Parameters

The analysis has assumed that the leachate drainage blanket will be free draining. Hence, the influence of pore water pressures is not applicable to this analysis, therefore within the input parameters detailed in Appendix II, the parallel submerged ratio is set to zero.

The assessment has considered 5 cases, for the loading of the lining system, these are detailed below:

- Case 1 - Lining system comprising clay liner, overlain by GCL, textured geomembrane and geotextile protector, is installed on a slope with a gradient of 1v : 1.5h. Directly above the geotextile a 500mm thick layer of granular drainage stone is placed to the full height of the slope, (i.e. a lift height of 10m).
- Case 2 - As Case 1, with the exception that the cohesive intercept between the clay liner and GCL has been reduced to model softening at this interface.
- Case 3 - As Case 2, but with a reduction in the cohesive intercept at the GCL / geomembrane interface.
- Case 4 - As Case 3, but with a reduced cohesive strength at the geomembrane / geotextile protector interface.
- Case 5 - As Case 4, but with a reduced angle of friction between the GCL and geomembrane.

4.0 Results

A full listing of the input parameters, derived forces and calculated results are presented in Appendix II. A summary of the results is presented Table 2.

Case 1 demonstrates that the factor of safety against failure at each interface is acceptable, assuming peak strength parameters as detailed in Table 1 for a 10m high slope. The lowest factor of safety being 1.8, for a failure solely within the drainage media.

To model the effects of softening at the interfaces, the cohesion for each interface assumed in Case 1, with the exception of the drainage stone / geotextile protector interface, have been reduced in Cases 2, 3 and 4. In these cases there is an expected reduction in the factor of safety at each interface as the cohesion is removed. However in all these cases lowest factor of safety of 1.35, occurs between the GCL and underlying clay liner. This factor of safety is still considered to be acceptable.

Case 5 assumes a lower angle of friction between the GCL and geomembrane in order to model possible migration of the bentonite through the geotextile of the GCL. Published data would suggest that the peak angle of friction for the GCL adopted for the analysis is conservative. Recent back analysis of a failure of a similar lining system to that proposed at Blessington indicated that the friction angle prior to failure was approximately 21°. Whilst the conditions experienced at the failed site would not be encountered at Blessington, it is considered suitable to consider this value as a worst case scenario for the investigation. By reducing the angle of friction between the GCL and geomembrane, the factor of safety at this interface is reduced to 1.17. Whilst this is lower than would normally be considered acceptable, given the worst-case assumptions made, a factor of safety in excess of 1.1 is considered acceptable.

Variable Input Parameter	Unit	Case 1	Case 2	Case 3	Case 4	Case 5
Slope Height	m	10	6	6	6	6
Angle of Shearing of Protection Layer	°	35	35	35	35	35
Friction Drainage Blanket / Geotextile	°	33	33	33	33	33
Cohesion of Blanket / Geotextile	kPa	0	0	0	0	0
Friction Drainage Geotextile / Geomembrane	°	26	26	26	26	26
Cohesion of Geotextile / Geomembrane	kPa	7	7	7	0	0
Friction Geomembrane / GCL	°	25	25	25	25	20
Cohesion of Geomembrane / GCL	kPa	2	2	0	0	0
Friction Drainage Geomembrane / GCL	°	23	23	23	23	23
Cohesion of Geomembrane/GCL	kPa	2	0	0	0	0
Factor of Safety Against Failure						
Drainage Blanket		1.80	1.80	1.80	1.80	1.80
Drainage Blanket / Geotextile interface		4.35	4.35	4.35	1.53	1.53
Geotextile / Geomembrane interface		2.27	2.27	1.47	1.47	1.17
Geomembrane / GCL interface		2.15	1.35	1.35	1.35	1.35
GCL / Subgrade interface						
Tension In Geosynthetic Material						
Geotextile		No	No	No	No	No
Geomembrane		No	No	No	No	No
GCL		No	No	No	No	No

Table 2 : Summary of Analysis.

5.0 Discussion and Recommendations

An analysis of the proposed lining system for the proposed engineered landfill at Blessington has been undertaken. The analysis has concentrated on the interface stability between the geosynthetic and soil elements of the lining system. In the analysis a gradient of 1v:3h and a maximum slope height of 10m have been assumed, in line with the proposed design. In the absence of site-specific test data, conservative parameters have been adopted for each of the interfaces and subsequently varied to investigate degradation of the interface. The analyses have demonstrated that the proposed lining system has an acceptable factor of safety for all the cases considered.

Some consideration must be given to the method of placement of the drainage blanket, as this could place additional forces on the geosynthetic materials. It is recommended that the drainage blanket is placed from the bottom up, with dump trucks tipping the drainage stone at the toe of the slope and with either a tracked excavator or low ground pressure dozer placing the material up the slope, to minimise any dynamic forces induced by moving plant.

References

Jones, D.R.V. and Dixon N. (1998) *The Stability of Geosynthetics in Landfill Lining Systems*, Proceedings of the Symposium on the Geotechnical Engineering of Landfills, 24 September

APPENDIX I

For inspection purposes only.
Consent of copyright owner required for any other use.

and this paper should be used as a guide only.
Geosynthetic clay liners (GCLs) are assembled from layers of synthetic materials and bentonite, and are used as primary and/or secondary liners in landfill applications. Gartung & Zanzinger present a comprehensive overview of the engineering properties and use of GCLs. The function and properties of GCLs, together with the importance of quality control are highlighted in the paper; which includes two case histories from Germany on performance observations from GCLs used in capping applications. At the Hamburg-Georgswerder site, problems of root damage, desiccation and cation exchange arose due to lack of sufficient soil cover. However, the second case history, at Nuremberg, reports a successful use of a GCL on a landfill capping system. The authors conclude with advice on the use of GCLs in landfill covers given by the German Institute of Construction; if this guidance is followed in the UK, desiccation can be avoided.

The stability of geosynthetic landfill lining systems

D.R.V. Jones⁽¹⁾ and N. Dixon⁽²⁾

1) Golder Associates, Landmere Lane, Nottingham NG12 4DG

2) The Nottingham Trent University, Nottingham NG1 4BU

Introduction

Geosynthetic materials are now commonly used in landfills for many applications such as:

- Geomembranes used as primary liners as barriers to leachate and landfill gas escape.
- Geotextiles used as separation layers, filter layers and as geomembrane protectors.
- Geosynthetic Clay Liners (GCLs) used as primary or secondary liners.
- Geonets and geocomposites used as leachate, landfill gas and groundwater drainage layers.
- Geogrids used for reinforcing applications.

The stability of a geosynthetic landfill lining system is controlled by the shear strength between the various interfaces, i.e. geosynthetic/geosynthetic and geosynthetic/soil interface shear strengths. This paper considers the stability of geosynthetics on landfill side slopes and in sloping capping applications by presenting a summary of available interface shear strength values from the literature, supplemented by testing carried out at The Nottingham Trent University. Design methods promoted by various authors are discussed and modifications suggested.

Background

The shear strength developed at a geosynthetic interface is dependent on both the normal stress applied to the interface and the displacement at the interface. Several authors (e.g. Seed *et al.*, 1988, Byrne 1994 *etc.*) have indicated that most geosynthetic interfaces are strain softening, i.e. they exhibit a reduction in shear

For inspection purposes only.
Consent of copyright owner required for any other use.

stress at displacements beyond peak strengths. Typically for each normal stress, the shear stress increases from the origin with increasing displacement until a peak value is achieved. Subsequent displacement results in a reduction in shear stress to a constant or residual value.

If the peak and residual strengths are plotted against the relevant normal stresses, the resulting failure envelope can be defined. A linear Coulomb-type failure envelope is usually obtained which defines the interface shear strength in terms of the friction angle (δ) and cohesion intercept (α). It should be noted that these parameters only define the failure envelope for the range of normal stresses tested and that extrapolation of both friction angle and cohesion intercept outside the range may not be representative. These interface shear strength parameters can be used to assess the stability of any slope containing a geosynthetic, using a conventional soil mechanics approach.

Measurement of interface shear strength

The measurement of geosynthetic interface shear strength can be carried out by three main methods; direct shear testing, ring shear testing and testing with a tilting table. Direct shear testing can be carried out in standard soil shear boxes with dimensions of 60 mm x 60 mm and 100 mm x 100 mm which can be regarded as index testing, or can be more performance-related using larger 300 mm x 300 mm and 300 mm x 400 mm direct shear apparatus. All direct shear apparatus have limited displacements and it has been shown (Jones, 1998) that even displacements of 100 mm may not mobilise the true residual interface shear strengths.

Ring shear testing can be carried out to investigate the true residual strengths since the apparatus can produce unlimited displacements. It should be recognised, however, that the direction of shearing in a ring shear test is not comparable to the field and thus true residual shear strengths may only be of academic interest and the large strain strengths obtained from a direct shear test in a 300 mm x 400 mm apparatus may be sufficient for design applications. In addition, ring shear testing should not be used to measure peak interface shear strengths (Dixon & Jones, 1995).

The third main method of measurement is the use of a tilting table which has been used predominantly in Europe. There is currently no consensus on the size of apparatus required to provide performance results and its use is limited to low normal stresses. It may be, however, that the tilting table may be more accurate in determining the behaviour of geosynthetic interfaces at low confining stress.

Interface shear strength values

The following paragraphs summarise a literature search carried out to investigate the range of shear strengths published for various geosynthetic interfaces. The results of the literature search have been supplemented by over 200 direct shear

tests carried out at The Nottingham Trent University (Jones, 1998). Peak and residual shear strengths have been plotted against the appropriate normal stress (Figures 1, 2 and 3) and linear regression has been used to generate the failure envelope for each interface. The peak and residual shear strength envelopes are given, together with the correlation coefficient (R^2) which gives a statistical determination of whether the assumed linear regression is strong; a perfect straight line fit giving an R^2 value of 1.0.

Smooth HDPE geomembrane

The results of testing on smooth HDPE geomembranes are presented in Figure 1 and a summary is given in Table 1 below.

Interface	Interface shear strength parameters					
	Peak			Residual		
	δ ($^\circ$)	α (kPa)	R^2	δ ($^\circ$)	α (kPa)	R^2
Geonet	9.0	1.0	0.74	6.9	1.8	0.80
Non-woven geotextile	9.8	-0.8	0.88	5.8	0.3	0.88
Sand	26.9	-4.0	0.90	16.2	0.0	0.95
Clay - undrained	10.3	7.1	0.48	2.3	15.0	0.09
Clay - drained	21.5	2.1	0.86	17.1	-6.1	0.97

Table 1 Summary of results for smooth HDPE geomembrane

The summary plot of shear stress vs. normal stress for a smooth geomembrane/geonet interface (Figure 1a) shows a scatter in data points with a poor straight line fit for both peak and residual conditions with R^2 values of 0.74 and 0.80 respectively. This linear regression gives a peak friction angle of 9.0° , which reduces to 6.9° at large displacements. This interface has low cohesion intercepts for both peak (1.0kPa) and residual (1.8kPa) conditions. For the smooth geomembrane/non-woven geotextile interface, a peak interface friction angle of 9.8° , reducing to 5.8° for residual conditions (Figure 1b) is calculated; there is negligible cohesion intercept for this interface. Both peak and residual conditions give strong straight line fits both with correlation coefficient values of 0.88, however there is still a degree of scatter in the results (Figure 1b).

The smooth geomembrane/sand interface has much higher shear strength than the two interfaces discussed above. The peak interface shear strength using linear regression is $\delta = 26.9^\circ$ and $\alpha = -4.0$ kPa, and there is a good straight line fit with $R^2 = 0.90$ (Figure 1c). The residual values give slightly less scatter and thus a higher correlation coefficient of 0.95, and a residual friction angle of 16.2° .

Testing of the interface shear strength between geosynthetics and cohesive soil is more difficult than the testing of geosynthetic/geosynthetic or geosynthetic/granular interfaces since there is the possibility of pore water pressures at the interface during shearing. Such

negative (suctions) and will lead to a decrease or increase in effective stress at the interface thus making the assessment of interface shear strength more difficult. The assessment of whether the results quoted in the literature are based on undrained or drained conditions is based on either the various authors' descriptions or on an interpretation of the shearing rates used by the current authors. It is considered that the results presented may not be true undrained or drained conditions and thus caution is required when assessing the results.

For undrained tests it may be that the interface shear strength will be dependent on the undrained shear strength of the clay. However, not all authors reported the clay strength and this makes any accurate assessment of the results difficult if not impossible. The scatter in results for smooth HDPE geomembrane/clay interface (Figure 1d) is not unexpected. Correlation coefficients of 0.48 and 0.09 for the peak and residual envelopes respectively demonstrate this scatter. There is a clear increase in shear strength with increasing normal stress with a peak interface shear strength parameters of $\delta = 10.3^\circ$ and $\alpha = 7.1$ kPa. However, the friction angle of the residual envelope is negligible ($\delta = 2.3^\circ$) and the cohesion intercept is 15.0 kPa.

For the drained case the smooth geomembrane/clay interface has less scatter than the undrained conditions (Figure 1e). This may be associated with no pore pressures at the interface or may be due to the lower number of data points available. Both peak and residual envelopes have strong correlation coefficients of 0.86 and 0.97 respectively, and the peak interface friction angle of 21.5° reduces to a residual value of 17.1° . The cohesion intercept reduces from 2.1 kPa for the peak to -6.1 kPa for the residual shear strength. Since the residual envelope is only based on four data points it is not considered to be representative.

Textured HDPE geomembrane

The results of testing on textured HDPE geomembranes are presented in Figure 2 and a summary is given in Table 2 below.

Interface	Interface shear strength parameters					
	Peak			Residual		
	δ (°)	α (kPa)	R^2	δ (°)	α (kPa)	R^2
Geonet	11.0	3.0	0.98	9.1	9.2	0.96
Non-woven geotextile	25.8	6.9	0.88	13.1	3.6	0.88
Sand	27.4	6.9	0.96	25.5	15.5	0.90
Clay - undrained	4.4	36.0	0.13	3.1	34.0	0.21
Clay - drained	10.7	26.7	0.93	-	-	-

Table 2 Summary of results for textured HDPE geomembrane

The information available on the interface shear strength between textured HDPE geomembranes and geonets is limited and this may be because

the increase in interface shear strength over and above the smooth geomembrane is marginal. Figure 2a summarises the available information, although there are only five data points for the peak strength and three points for the residual strength. The peak interface shear strength based on this data is $\delta = 11.0^\circ$ and $\alpha = 3.0$ kPa with a correlation coefficient of 0.98, which compares with a friction angle of 9.0° for the smooth geomembrane case (Figure 1a). The residual interface shear strength for the textured geomembrane ($\delta = 9.1^\circ$ and $\alpha = 9.2$ kPa) needs to be treated with care since it is only based on three data points.

The majority of data presented for the shear strength of textured geomembrane/non-woven geotextile interfaces are from the results of the testing carried out by the authors (Jones & Dixon, 1998), although other information from the literature has been used to develop Figure 2b. A peak friction angle of 25.8° is obtained together with a cohesion intercept of 6.9 kPa, which reduces to residual values of $\delta = 13.1^\circ$ and $\alpha = 3.6$ kPa, although there is a significant range of values with R^2 values of 0.88 for both the peak and residual case.

The interface shear strength results for the textured geomembrane/sand interface are shown on Figure 2c which give peak parameters of $\delta = 27.4^\circ$ and $\alpha = 6.9$ kPa with a correlation coefficient of 0.96. This interface, although strain softening, does not seem to exhibit a large reduction in shear strength with increased displacement since the residual friction angle is 25.5° with a relatively high cohesion intercept of 15.5 kPa.

From the results of undrained tests on textured HDPE geomembrane against clays (Figure 2d), it can be seen that the dependency of shear strength on normal stress is limited with peak and residual friction angles of 4.4° and 3.1° respectively. Cohesion intercepts for both peak and large strain conditions are similar with a peak value of 36.0 kPa and a residual value of 34.0 kPa, however both envelopes give poor linear relationships with R^2 values of 0.13 and 0.21. The shape of the envelopes suggest that the shear strength between textured geomembrane and a clay tested without an allowance for the dissipation of pore pressures is almost independent of normal stress, and is likely to be related to the undrained shear strength of the clay. Since the data shown on Figure 2d has been obtained from eight separate references with different clay at different remoulding conditions, the extent of the data scatter is not surprising.

The results shown on Figure 2d compare well with the observations made by Orman (1994), who found that failure of a textured HDPE geomembrane/silt interface occurred within the silt along the line of the asperities on the geomembrane sheet. Thus it is to be expected that the undrained interface shear strength of a textured geomembrane/clay is independent of normal stress and probably equal to the undrained shear strength of the clay.

There is little information on geomembrane/clay interfaces tested at strain rates slow enough to dissipate pore waters pressures although the available data indicates that the shear strength of this interface is dependent on normal stress (Figure 2e). Again the small amount of data available means that caution is required when analysing the results however...

interface shear strength corresponding to $\delta = 10.7^\circ$ and $\alpha = 26.7$ kPa. Closer inspection of the plot reveals that a non-linear fit may be more representative for the peak shear strength envelope, possibly curving downwards at lower normal stresses and passing through the origin. There is insufficient data to determine the residual shear strength for this interface, however, it is likely that the residual interface shear strength will be the residual shear strength of the clay. The asperities of the textured geomembrane are very similar to the upper sintered brass platten on the standard Bromhead ring shear apparatus (Bromhead 1979).

Non-woven geotextile

The results of testing on non-woven geotextiles are presented in Figure 3 and a summary is given in Table 3 below.

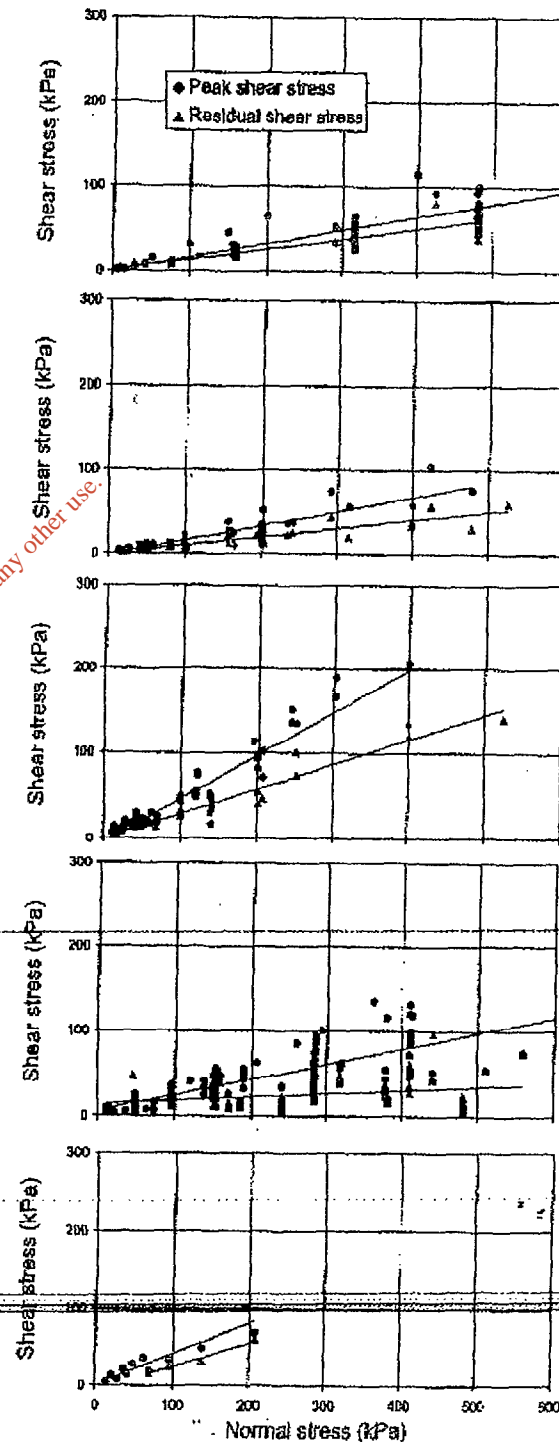
Interface	Interface shear strength parameters					
	Peak			Residual		
	δ ($^\circ$)	α (kPa)	R^2	δ ($^\circ$)	α (kPa)	R^2
Geonet	13.1	17.9	0.76	15.4	4.1	0.92
Gravel	35.0	-1.0	0.87	19.9	30.1	0.99
Sand	33.0	-1.3	0.93	28.7	7.7	0.92
Clay - undrained	25.3	5.3	0.91	17.7	55.6	0.98
Clay - drained	32.5	4.4	0.98	-	-	-

Table 3 Summary of results for non-woven geotextile

The results of shear strength testing on non-woven geotextile/geonet interfaces are plotted in Figure 3a and linear regression of all the data points give peak interface shear strengths of $\delta = 13.1^\circ$ and $\alpha = 17.9$ kPa with an R^2 value of 0.76. For the range of normal stresses considered, the residual envelope is similar to the peak in terms of its mobilised shear strength, however the friction angles and cohesion intercept are different. The best fit line through the residual data points is given by $\delta = 15.4^\circ$ and $\alpha = 4.1$ kPa, i.e. a higher friction angle but a lower cohesion intercept with a correlation coefficient of 0.92.

The non-woven geotextile/gravel interface has a high shear strength with some values in the literature reported as high as 48° . Most of the results available are for tests carried out at normal stresses less than 200 kPa (Figure 3b) and linear regression gives a friction angle of 35.0° with a cohesion intercept of -1.0 kPa. This reduces to a residual shear strength corresponding to $\delta = 19.9^\circ$ and $\alpha = 30.1$ kPa. The peak shear strength envelope shows a reasonable strong straight line fit with a correlation coefficient of 0.94, while the residual envelope has a very strong fit with $R^2 = 0.99$ however the residual is based on a small number of data points.

There is much more information available in the literature on the interface shear strength between sand and non-woven geotextiles, and this is also a high strength interface with a peak friction angle of 33.0° and a cohesion intercept of 1.3 kPa (Figure 3c). The residual shear strength for this interface is



(a) Geonet

(b) Non-woven Geotextile

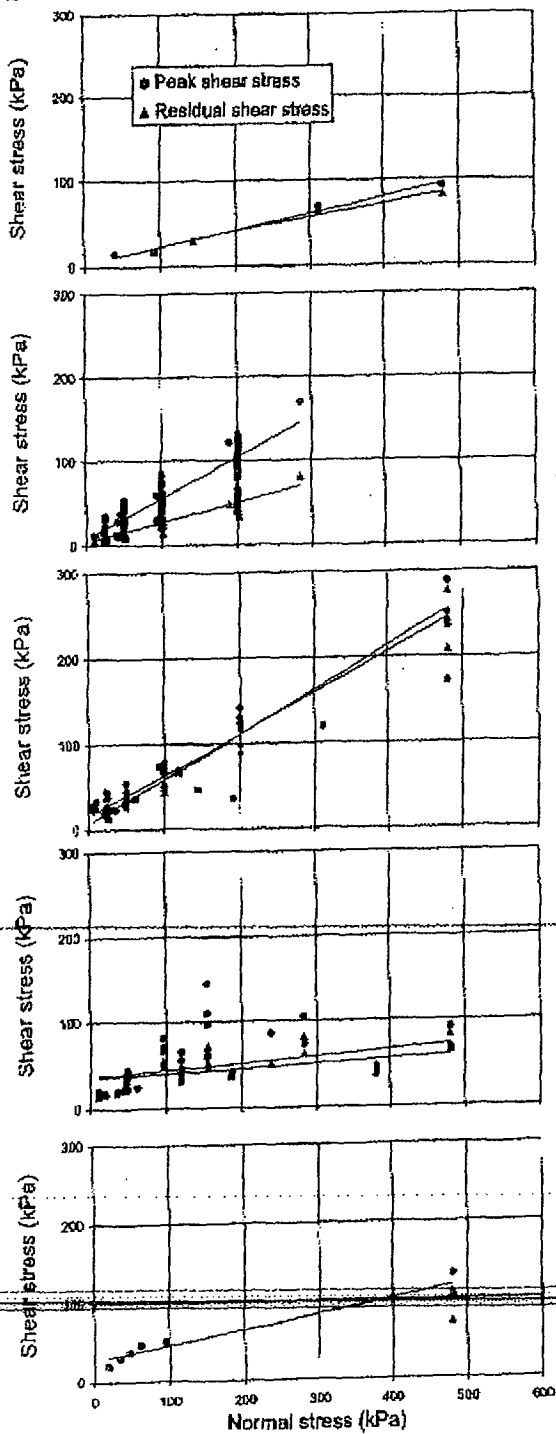
(c) Sand

(d) Clay - undrained

(e) Clay - drained

For inspection purposes only. Copyright owner required for any other use.

Geotechnical engineering of landfills



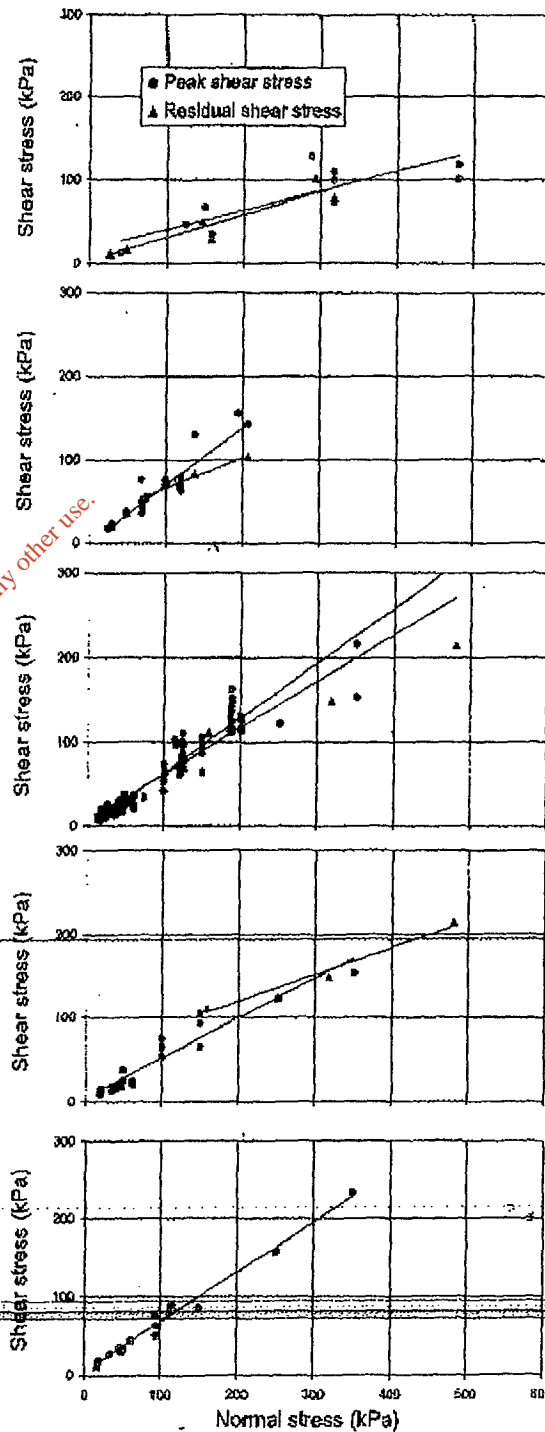
(a) Geonet

(b) Non-woven Geotextile

(c) Sand

(d) Clay - undrained

(e) Clay - drained



(a) Geonet

(b) Gravel

(c) Sand

(d) Clay - undrained

(e) Clay - drained

Figure 3 Non-woven Geotextile

For inspection purposes only.
Consent of copyright owner required for any other use.

reduced to a value of $\delta = 28.7^\circ$ and $\alpha = 7.7$ kPa. The peak interface shear strength envelope has been generated from over a hundred data points and the scatter is minimal with an R^2 value of 0.91. Less data was available for the residual plot, however the amount of scatter is less with a correlation coefficient of 0.98.

The results of undrained tests on non-woven geotextile/clay interface shown on Figure 3d. Peak interface shear strengths of $\delta = 25.3^\circ$ and $\alpha = 5.3$ kPa are obtained with a correlation coefficient of 0.91, which reduce to $\delta = 17.7^\circ$ and $\alpha = 55.6$ kPa for large strains. The residual envelope is based on three data points, has an extremely high cohesion intercept and has an R^2 value of 0.98. The peak interface shear strength is predominantly frictional in nature however the high cohesion intercept of the residual envelope could be indicative of dependence on the undrained shear strength of the clay. In particular it may be that the failure plane exists in the outer layer of the geotextiles' fibres which are clay filled, and thus the shear strength is a combination of the fibres' frictional (and possibly tensile) strength together with the clay's strength.

A higher shear strength is obtained for drained tests on non-woven geotextile/clay interfaces, as shown on Figure 3e. The summary plot of all data points gives a good straight line fit ($R^2 = 0.98$) for the peak interface shear strength with a high friction angle of 32.5° and a cohesion intercept of 4.4 kPa. There is insufficient information to generate a residual interface shear strength envelope.

Overview of stability analysis from the literature

In considering the stability of a slope lined with geosynthetics, several failure mechanisms need to be assessed. Conventional limit equilibrium methods such as Bishop (1955) and Janbu (1973) or approximate methods such as the charts proposed by Taylor (1937) can be used to assess the overall stability of the host slope. The use of geosynthetics often introduce potentially weak planes into the system and require special consideration.

The stability of a cover soil above the geosynthetics was discussed by Martin & Koerner (1985), and using an infinite slope approach presented the factor of safety against the failure of a uniform cover soil as:

$$F = \frac{\tan \delta}{\tan \beta} \tag{Equation 1}$$

where δ is the friction angle between the geosynthetic and cover soil,
 β is the slope angle.

The above equation applies when the cover soil is dry or subjected to an external hydrostatic water pressure distribution. However, such conditions where there is external water pressures are normally restricted to ponds and reservoirs, and it is more useful to consider active seepage in the cover soil. For

full depth seepage, Martin & Koerner (1985) suggest an approach based on a reduction in effective normal stress on the liner, i.e.

$$F = \frac{\gamma_b \tan \delta}{\gamma_s \tan \beta} \tag{Equation 2}$$

where γ_b is the buoyant unit weight of cover soil
 γ_s is the saturated unit weight of cover soil

Note that $\gamma_b = \gamma_s - \gamma_w$, where γ_w is the unit weight of water. This is a conservative approximation and assumes that the water pressures are calculated using vertical depth below ground level.

Giroud & Beech (1989) give two reasons why a finite slope is more stable than an infinite slope assumed in the analysis method described above; the presence of a geosynthetic anchorage at the crest, and the buttressing effect of the soil at the base of the slope. As slippage along the critical geosynthetic interface occurs, tensile forces are generated in the geosynthetics above the critical interface, and these tensile forces contribute to the stability of the potential sliding block. The authors summarise the three factors contributing to the lining's stability as:

- Geosynthetic tension resulting from the crest anchorage.
- Shear resistance developed along the interface.
- Toe buttressing effect.

In their limiting equilibrium method, Giroud & Beech (1989) proposed dividing the system into two wedges and forces that are balanced in the vertical and horizontal directions. This method provides two equilibrium equations and three unknowns, and an iterative process is required to provide a solution. A major drawback with this method is that the distribution of tensile stresses within the geosynthetic layers cannot be determined. Koerner & Hwu (1991) proposed a limiting equilibrium method also based on the two part wedge method, and considered sliding of the active wedge to be resisted by only the shear strength along the geosynthetic/cover soil interface and the passive soil wedge buttress at the toe of the slope. The factor of safety (F) with respect to sliding of the system is a solution of the following quadratic equation:

$$aF^2 + bF + c = 0 \tag{Equation 3}$$

where,

$$a = \frac{\gamma_h L}{2} \sin^2(2\beta) \tag{Equation 4}$$

$$b = -[\gamma_h L \cos^2 \beta \tan \delta_s \sin(2\beta) + \alpha_s L \cos \beta \sin(2\beta) + \gamma_h L \sin^2 \beta \tan \phi \sin(2\beta) + 2ch \cos \beta + \gamma_h^2 \tan \phi] \tag{Equation 5}$$

$$c = (\gamma_h L \cos \beta \tan \delta_u + \alpha_u L)(\tan \phi \sin \beta \sin(2\beta)) \tag{Equation 6}$$

- and,
- γ unit weight
- h thickness of cover soil (measured perpendicular to slope)
- L slope length
- β slope angle
- ϕ angle of internal friction of cover soil
- c cohesion of cover soil
- δ_u interface friction angle at the upper interface
- α_u apparent cohesion at upper interface

This approach assumes that the factor of safety is the same value at every point along the sliding surface defined by the two wedge mechanism. By default this means that the factor of safety is the same with respect to the shearing resistance at the active wedge/geosynthetic interface as that with respect to the shearing resistance of the cover soil beneath the passive wedge. Koerner & Hwu (1991) further proposed a model to assess the tension in a geosynthetic due to unbalance interface shear forces. By assuming uniform mobilisation of the interface shear strengths along the geomembrane, they developed an expression for the tensile force per unit width of slope as follows:

$$T = [(\alpha_u - \alpha_l) + \gamma h \cos \beta (\tan \delta_u - \tan \delta_l)] L \quad \text{Equation 7}$$

where,

- δ_l interface friction angle at the lower interface
- α_l apparent cohesion at lower interface

This equation expresses the imbalance between the maximum shear force that can act at the geosynthetic upper interface and the maximum shear force at the lower interface. When the upper shear force is smaller than the force at the lower surface the geosynthetic is in equilibrium and is not stressed. However, when the upper shear force is greater than the lower, a tensile force T is required in the geomembrane to ensure equilibrium. A major shortcoming with this method is that the tensile force computed is independent of the level of shear stress effectively mobilised at the upper interface. The shear force at the upper interface in this equation should be the mobilised shear force. Bourdeau *et al.* (1993) proposed a coupling between Equations 3 and 7 by replacing the ultimate upper shear strength with a mobilised value calculated by dividing the ultimate value by the factor of safety calculated in Equation 3, i.e. replacing $\alpha_u + \gamma h \cos \beta \tan \delta_u$

by
$$\frac{\alpha_u + \gamma h \cos \beta \tan \delta_u}{F}$$

which gives a new expression for the tensile force in the geosynthetic:

$$T = \left[\left(\frac{\alpha_u}{F} - \alpha_l \right) + \gamma h \cos \beta \left(\frac{\tan \delta_u}{F} - \tan \delta_l \right) \right] L \quad \text{Equation 8}$$

For a multi-layered system, the limit method proposed by Koerner (1990) can be used to determine the tensile forces in subsequent lower layers. This is a force equilibrium procedure which balances forces in the direction parallel to the slope. The shear force mobilised in the upper surface of a geosynthetic is transferred to its lower surface by shear until the maximum shear strength of that interface has been reached, and the remaining force will be taken in tension in the geosynthetic.

The above methods do not consider the effect of seepage forces on the stability of a cover soil. Soong & Koerner (1995) have developed a model that considers seepage flow parallel to the slope, i.e. a flow net within the cover soil mass consists of flow lines parallel to the slope and equipotential lines perpendicular to the slope. They produce two models for stability assessment; one for the case of a horizontal seepage build-up and one for a parallel-to-slope seepage build-up. The second model only will be considered below.

The expression developed by Soong & Koerner (1995) for the factor of safety against sliding of a cover soil on a geosynthetic can also be represented by a quadratic equation (Equation 3) with the following constants:

$$a = W_A (\sin \beta) (\cos \beta) - U_h (\cos^2 \beta) + U_h \quad \text{Equation 9}$$

$$b = -W_A (\sin^2 \beta) (\tan \phi) + U_h (\sin \beta) (\cos \beta) (\tan \phi) - N_A (\cos \beta) (\tan \delta) - (W_P - U_v) (\tan \phi) \quad \text{Equation 10}$$

$$c = N_A (\sin \beta) (\tan \delta) (\tan \phi) \quad \text{Equation 11}$$

For the case of parallel-to-slope seepage build-up, the constants in the above equations are given by:

$$W_A = \frac{[\gamma_d (h - h_w) (2H \cos \beta - (h + h_w)) + \gamma_{sat} h_w (2H \cos \beta - h_w)]}{\sin(2\beta)}$$

$$W_P = \frac{[\gamma_d (h^2 - h_w^2) + \gamma_{sat} h_w^2]}{\sin(2\beta)}$$

$$U_h = \frac{[\gamma_w h_w \cos \beta (2H \cos \beta - h_w)]}{\sin(2\beta)}$$

$$U_h = \frac{\gamma_w h_w^2}{2}$$

$$N_A = W_A \cos \beta + U_h \sin \beta - U_n$$

$$U_v = \frac{U_b}{\tan \beta}$$

- where
- W_A = total weight of the active wedge
 - W_P = total weight of the passive wedge
 - U_n = resultant of the pore pressures acting perpendicular to the slope
 - U_h = resultant of the pore pressures acting on the interwedge surfaces
 - U_v = resultant of the vertical pore pressures acting on the passive wedge
 - N_A = effective force normal to the failure plane of the active wedge
 - γ_d = dry unit weight of the cover soil
 - γ_{sat} = saturated unit weight of the cover soil
 - h_w = thickness of saturated cover soil (measured perpendicular to slope)

It should be noted that for the case of parallel-to-slope seepage build-up, the ratio of h_w/h can be defined by the parallel submergence ratio, PRS.

Proposed stability analysis methodology

Soong & Koerner (1995) consider a granular cover soil with an internal friction angle of ϕ , and in the consideration of seepage forces this is satisfactory. In addition, the interface shear strength between the upper geosynthetic and the cover soil is only represented by a friction angle (δ). In an attempt to make this approach more generic, the effect of a cover soil with cohesion (c) and an interface with a cohesion intercept of α , the equations have been re-written to include these terms. The inclusion of these parameters will change the b and c terms in the quadratic equation as follows:

$$b = \frac{-[W_A \sin^2 \beta \tan \phi] + [U_h \sin \beta \cos \beta \tan \phi]}{[\cos \beta (\alpha L + N_A \tan \delta)] - [(W_P - U_v) \tan \phi]} \left[\frac{ch}{\sin \beta} \right]$$

Equation 12

$$c = \sin \beta \tan \phi (\alpha L + N_A \tan \delta)$$

Equation 13

Further, the stress normal to the interface used in the calculation of the geosynthetic tensile force (Equation 8) should take account of the piezometric surface. This equation now becomes:

$$T = \left[\left(\frac{\alpha_n}{F} - \alpha_1 \right) + (\gamma_{sat} h_w + \gamma_d (h - h_w)) \cos \beta \left(\frac{\tan \delta_n}{F} - \tan \delta_1 \right) \right] L$$

Equation 14

It is proposed that the stability of a cover soil over several layers of geosynthetics together with the tension developed in the geosynthetics can be established as follows:

1. Calculate the factor of safety against cover soil sliding using the approach of Soong & Koerner (1995), modified to allow for c and α .
2. Calculate the mobilised tension in the upper geosynthetic using Bourdeau *et al.* (1993) with the modification for γ_{sm} and γ_b .
3. Calculate the mobilised tension in the remaining geosynthetics.

Example 1

This methodology is used in the following example. Consider the stability of a landfill capping system comprising 1 m of gravelly cover soil resting on a non-woven geotextile protection over a 1mm thick smooth HDPE geomembrane. A blinding layer of sand has been placed beneath the geomembrane. The maximum slope height is 20 m and the slope gradient is 1:3 (18.4°). The following internal strengths and interface shear strengths (obtained from Tables 1, 2 and 3) apply:

Cover soil:	$\phi = 35^\circ, c = 0 \text{ kPa}$
Cover soil/geotextile:	$\delta = 35^\circ, \alpha = 0 \text{ kPa}$
Geotextile/smooth geomembrane:	$\delta = 10^\circ, \alpha = 0 \text{ kPa}$
Smooth geomembrane/sand:	$\delta = 27^\circ, \alpha = 0 \text{ kPa}$

The cover soil has a dry unit weight of 18 kN/m^3 , and a saturated unit weight of 21 kN/m^3 . Consider a case of a parallel submergence ratio of 0.25.

The length of the slope is given by:

$$L = \frac{H}{\sin \beta} = \frac{20}{\sin 18.4} = 63.36 \text{ m}$$

Also, the height of water in the cover soil (perpendicular to the slope) is:

$$h_w = \text{PRS} \times h = 0.25 \times 1.0 = 0.25 \text{ m}$$

For inspection purposes only
Consent of copyright owner required for any other use

1. Calculate the factor of safety against sliding

First calculate the constants:

$$W_A = \frac{18(1.0 - 0.25)(2 \times 20 \cos 18.4 - (1.0 + 0.25)) + 21 \times 0.25(2 \times 20 \cos 18.4 - 0.25)}{\sin(2 \times 18.4)}$$

$$W_A = \frac{495.52 + 197.95}{0.599} = 1157.71 \text{ kN}$$

$$W_P = \frac{18(1^2 - 0.25^2) + 21 \times 0.25^2}{0.599} = 30.36 \text{ kN}$$

$$U_n = \frac{10 \times 0.25 \cos 18.4 (2 \times 20 \cos 18.4 - 0.25)}{0.599} = 149.32 \text{ kN}$$

$$U_b = \frac{10 \times 0.25^2}{2} = 0.31 \text{ kN}$$

$$N_A = 1157.71 \cos 18.4 + 0.31 \sin 18.4 - 149.32 = 949.30 \text{ kN}$$

$$U_v = \frac{0.31}{\tan 18.4} = 0.93 \text{ kN}$$

From Equation 9:

$$a = 1157.71 \sin 18.4 \cos 18.4 - 0.31 \cos^2 18.4 + 0.31$$

$$a = 346.78$$

From Equation 12:

$$b = \frac{-[1157.71 \sin^2 18.4 \tan 35] + [0.31 \sin 18.4 \cos 18.4 \tan 35]}{[\cos 18.4 (0 + 949.30 \tan 35)]}$$

$$b = \frac{-[(30.36 - 0.93) \tan 35] - [0]}{-732.03}$$

From Equation 13:

$$c = \sin 18.4 \tan 35 [0 + 949.30 \tan 35]$$

$$c = 146.91$$

Now calculate factor of safety from:

$$F = \frac{-b + \sqrt{b^2 - 4ac}}{2a}$$

$$F = \frac{-(-732.03) + \sqrt{(-732.03)^2 - 4 \times 346.78 \times 146.91}}{2 \times 346.78}$$

$$F = \frac{732.03 + 576.27}{693.56}$$

$$F = 1.89$$

2. Calculate mobilised tension in upper geosynthetic (geotextile)

From Equation 14:

$$T = \frac{[(0 - 0) + (21 \times 0.25 + 18(1 - 0.25)) \cos 18.4 \left(\frac{\tan 35}{1.89} - \tan 10 \right)]}{63.36}$$

$$T = \frac{[0 + 17.79 \left(\frac{\tan 35}{1.89} - \tan 10 \right)]}{63.36}$$

$$T = 218.84 \text{ kN}$$

It is unlikely that the tensile strength of a non-woven geotextile will withstand this tension and it will lead to failure of the geotextile in tension and sliding of the cover soil and geotextile on the geomembrane. There will therefore not be any tension in the geomembrane since failure will occur above it.

Example 2

Now consider the same case as above but this time the smooth geomembrane is replaced by a textured geomembrane. The relevant interface shear strength parameters are:

Geotextile/textured geomembrane: $\delta = 26^\circ$, $\alpha = 7 \text{ kPa}$

Textured geomembrane/sand: $\delta = 27^\circ$, $\alpha = 7 \text{ kPa}$

Since the upper geosynthetic remains the same, the calculated factor of safety remains the same. The tension in the geotextile is obtained from Equation 14:

$$T = \frac{[(0 - 7) + 17.79 \left(\frac{\tan 35}{1.89} - \tan 26 \right)]}{63.36}$$

$$T = -575.68 \text{ kN}$$

Since T is negative, the shear strength of the lower interface is greater than the mobilised shear stress on the upper interface and there is no tension in the geotextile. The mobilised shear stress is thus transferred from the geotextile to the geomembrane with no tension induced in the geotextile. Now check if there is any tension in the geomembrane:

$$T = \frac{\left[\left(\frac{7}{1.89} - 7 \right) + 17.79 \left(\frac{\tan 26}{1.89} - \tan 27 \right) \right]}{63.36}$$

$$T = \frac{[-3.30 - 4.47]}{63.36}$$

$$T = -492.30 \text{ kN}$$

Hence the geomembrane can also transfer the shear stress to the sand below without any tension.

For inspection purposes only. Consent of copyright owner required for any other use.

Page 10/11
21-Apr-04 15:36
v:\r\pouzi\

Discussion

Interface shear strength

The interface shear strength parameters given in this paper have been taken from technical papers available in the literature, in-house testing carried out by Golder Associates in north America and testing carried out at The Nottingham Trent University. The testing was generally carried out in direct shear apparatus of varying size, together with ring shear testing to obtain some of the residual shear strength parameters. The geosynthetics and soils used in the testing vary widely and caution should be exercised when using the data presented in Tables 1 to 3. It is suggested that these values may be used in preliminary designs, however the authors stress the importance of site specific performance testing. In particular, the mean values of friction angle and cohesion intercept presented are taken from tests carried out at normal stresses over a range up to 600 kPa. The values presented in this paper may not be reliable for the design of landfill capping systems and other applications with low normal stresses.

The friction angle and cohesion intercept obtained from any interface shear strength testing are simply parameters that describe the failure envelope for the range of normal stresses used. In other words, they describe the position of the best fit line through the data. A reported cohesion intercept does not necessarily imply that there is a shear strength under zero normal load, although some interfaces, e.g. textured geomembrane/non-woven geotextile and internal strength of geocomposites, will have an actual strength at zero load due to either the mingling of geotextile fibres within the asperities of the geomembrane or from bonding between various layers of a geocomposite. It is up to the judgement of the engineer as to what allowance is made for the cohesion intercept in a design situation.

Stability analysis

The method presented in this paper expands on the work of others as described above. It may be for the case of capping systems that this simple limiting equilibrium method will give satisfactory results. In the case of a landfill side slope, however, the settlement of the waste will induce displacements at the interfaces. In order to model these conditions, numerical techniques can be used (Jones, 1998) to quantify the mobilised shear stresses in the system. If such analyses cannot be justified then the authors would recommend that the design engineer uses peak interface shear strength values on the base on the landfill only, and that consideration should be given to using residual shear strengths along the side slopes.

Acknowledgements

The laboratory testing carried out at The Nottingham Trent University was funded by Golder Associates (UK) Ltd. and the EPSRC as part of the Teaching Company Scheme (Grant Ref. GR/R5721). The testing was carried out by the

acknowledged. Materials used in the testing programme were provided by GSE Environmental and Geofabrics Ltd, and thanks are due to these suppliers.

References

- Bishop, A.W. (1955). The use of the slip circle in the stability analysis of earth slopes, *Geotechnique*, 5, 7-17.
- Bourdeau, P.L., Ludlow, S.J. & Simpson, B.E. (1993). Stability of Soil-Covered Geosynthetic-Lined Slopes: A Parametric Study, *Proc. Geosynthetics '93*, Vancouver, Canada, 1511-1521.
- Bromhead, E.N. (1979). A simple ring shear apparatus, *Ground Engineering*, 12, 5, 40-44.
- Byrne, R.J. (1994). Design issues with strain softening interfaces in landfill liners, *Proc. Waste Tech '94*, Charleston, South Carolina, USA, Session 4, Paper 4.
- Dixon, N. & Jones, D.R.V. (1995). Discussion on "Landfill liner interface strengths from torsional-ring shear tests", *Journal of Geotechnical Engineering*, ASCE, 121, 6, 509-510.
- Giroud, J.P. & Beech, J.F. (1989). Stability of Soil Layers on Geosynthetic Lining Systems, *Proc. Geosynthetics '89*, San Diego, USA.
- Janbu, N. (1973). Slope stability computations in embankment dam engineering, *Casagrande memorial volume*, eds Hirschfield & Poulos, John Wiley, New York, 47-86.
- Jones, D.R.V. (1998). The stability of geosynthetic landfill lining systems, PhD thesis in prep., The Nottingham Trent University.
- Jones, D.R.V. & Dixon, N. (1998). Shear strength properties of geomembrane/geotextile interfaces, *Geotextiles and Geomembranes* (in press.)
- Seed, R.B., Mitchell, J.K. & Seed, H.B. (1988). Slope stability failure investigation: Landfill Unit B-19, Phase 1-A, Kettleman Hills, California, *Report No. UCB/GT/88-01*, Dept. of Civil Engineering, University of California, Berkeley.
- Koerner, R.M. (1990). *Designing with Geosynthetics*, Second Edition, Prentice Hall, Englewood Cliffs, NJ.
- Koerner, R.M. & Hwu, B-L. (1991). Stability and tension considerations regarding cover soils in geomembrane lined slopes, *Geotextiles and Geomembranes*, 10, 4, 335-355.
- Martin, J.P. & Koerner, R.M. (1985). Geotechnical Design Considerations for Geomembrane Lined Slopes: Slope Stability, *Geotextiles and Geomembranes*, 2, 229-321.
- Orman, M.E. (1994). Interface Shear Strength Properties of Roughened HDPE, *Journal of Geotechnical Engineering*, ASCE, 120, 4, 758-761.
- Soong, T-Y & Koerner, R.M. (1995). Seepage Induced Slope Instability, *Proc. 9th GRI Conference*, Philadelphia, USA.
- Taylor, D.W. (1937). Stability of earth slopes, *J. Boston Soc. Civil Engrs.*, 24, 107-116.

APPENDIX II

For inspection purposes only.
Consent of copyright owner required for any other use.

SITE: Proposed Engineered Landfill, Blessington

Lining System Interface Stability

Input Parameters

			Case 1	Case 2	Case 2	Case 3	Case 4
β	Slope Angle	°	18.60	18.60	18.60	18.60	18.60
H	Slope height	m	9.00	9.00	9.00	9.00	9.00
h	Thickness of cover soils	m	0.50	0.50	0.50	0.50	0.50
ϕ	Friction angle of cover soil	°	35.00	35.00	35.00	35.00	35.00
c	Cohesion of cover soil	kPa	0.00	0.00	0.00	0.00	0.00
δ_{ct}	Interface friction angle Stone/Geotextile interface	°	30.00	30.00	30.00	30.00	30.00
α_{ct}	Apparent cohesion of Stone/Geotextile interface	kPa	0.00	0.00	0.00	0.00	0.00
δ_{tg}	Interface friction angle Textile/Geomembrane interface	°	26.00	26.00	26.00	26.00	26.00
α_{tg}	Apparent cohesion of Textile/Geomembrane interface	kPa	7.00	7.00	7.00	0.00	0.00
δ_{gs}	Interface friction angle Geomembrane/GCL interface	°	25.00	25.00	25.00	25.00	20.00
α_{gs}	Apparent cohesion of Geomembrane/GCL interface	kPa	2.00	2.00	0.00	0.00	0.00
δ_{gs}	Interface friction angle GCL/Clay interface	°	23.00	23.00	23.00	23.00	23.00
α_{gs}	Apparent cohesion of GCL/Clay interface	kPa	2.00	0.00	0.00	0.00	0.00
PRS	Parallel Submerged Ratio		0.00	0.00	0.00	0.00	0.00
γ_d	Dry unit weight of cover soil	kN	16.00	16.00	16.00	16.00	16.00
γ_{sat}	Saturated weight of cover soil	kN	18.00	18.00	18.00	18.00	18.00
h_w	Thickness of saturated cover soil	m	0.00	0.00	0.00	0.00	0.00
W_A	Weight of active wedge	kN	219.12	219.12	219.12	219.12	219.12
W_P	Weight of passive wedge	kN	6.62	6.62	6.62	6.62	6.62
U_n	Resultant pore water pressure perpendicular to slope	kN	0.00	0.00	0.00	0.00	0.00
U_h	Resultant pore water pressure on interwedge surface	kN	0.00	0.00	0.00	0.00	0.00
N_{Aab}	Effective force normal to failure plane of active wedge above impermeable layer	kN	207.67	207.67	207.67	207.67	207.67
N_{Abb}	Effective force normal to failure plane of active wedge below impermeable layer	kN	207.67	207.67	207.67	207.67	207.67
U_v	Resultant vertical pore water pressure acting on passive wedge	kN	0.00	0.00	0.00	0.00	0.00
L	Slope Length	m	28.22	28.22	28.22	28.22	28.22

Soils/Geotextile Interface

Quadratic Equation Parameters	a	66.24	66.24	66.24	66.24	66.24
	b	-133.88	-133.88	-133.88	-133.88	-133.88
	c	26.78	26.78	26.78	26.78	26.78
Factor of Safety Against Failure		1.80	1.80	1.80	1.80	1.80
Tension in Protection Geotextile	kN	-233.09	-233.09	-233.09	-35.57	-35.57

No Tension No Tension No Tension No Tension No Tension

Geotextile/Geomembrane Interface

Quadratic Equation Parameters	a	66.24	66.24	66.24	66.24	66.24
	b	-303.44	-303.44	-303.44	-116.24	-116.24
	c	66.73	66.73	66.73	22.62	22.62
Factor of Safety Against Failure		4.35	4.35	4.35	1.53	1.53
Tension in Geomembrane	kN	-86.79	-86.79	-30.36	-31.65	-9.75

No Tension No Tension No Tension No Tension No Tension

Geotextile/Geomembrane Interface

Quadratic Equation Parameters	a	66.24	66.24	66.24	66.24	66.24
	b	-165.51	-165.51	-112.02	-112.02	-91.88
	c	34.23	34.23	21.63	21.63	16.88
Factor of Safety Against Failure		2.27	2.27	1.47	1.47	1.17
Tension in Geomembrane	kN	-111.33	-54.90	-67.88	-25.69	-39.98

No Tension No Tension No Tension No Tension No Tension

Geomembrane/Subgrade Interface

Quadratic Equation Parameters	a	66.24	66.24	66.24	66.24	66.24
	b	-157.28	-103.79	-103.79	-103.79	-103.79
	c	32.29	19.69	19.69	19.69	19.69
Factor of Safety Against Failure		2.15	1.35	1.35	1.35	1.35

N.B. This calculation assumes friction angles and cohesion as published in the Loughborough University report.